Lasers in Manufacturing Conference 2019

High-Speed Imaging investigation of Laser Metal Deposition with various beam profiles

Himani Siva Prasad[a*], Frank Brueckner[b], Alexander Kaplan[a]

[a] *Department of Engineering Sciences and Mathematics, Luleå University of Technology, 971 87 Luleå, Sweden*
[b] *Fraunhofer IWS, Winterbergstrasse 28, 01277 Dresden, Germany*

Abstract

Laser Metal Deposition (LMD) of a high deposition rate process using a coaxial nozzle is investigated through high-speed imaging and metallographic analysis. The influences of using top-hat and doughnut laser beam profiles are compared. An island of unmelted powder develops in the centre of the laser spot, for example because of a well-focused powder stream. When cladding is performed in a single direction, the melt pool is smaller and the powder island is larger for the doughnut in comparison to the top-hat profile. This difference is reduced on using a meander cladding path. For both cladding paths, the dilution is more even in the case of the top-hat beam. Other observations about melt pool flows, solidification, powder catchment and incorporation are made from the high-speed videos.

Keywords: Laser Metal Deposition; Laser cladding; High-speed imaging; high deposition rate; beam shapes

1. Introduction

Laser Metal Deposition (LMD) is an additive manufacturing process where material is deposited layer by layer to produce a near net shaped component. A high power laser beam is used to create a melt pool on the substrate into which a feedstock material, metal powder for example, is fed. This method can be used to produce three dimensional components or clads in a single layer, also called laser cladding, for example to adjust properties such as wear resistance, corrosion etc.

Dilution from the base material into the cladding material is to be kept low to retain its properties. Through the use of laser cladding, dilution can be limited to as low as 2 % (Koshy, 1985).

Various cladding strategies (or deposition patterns) can be used to apply the clad layer. Some examples are a raster or spiral patterns. Since thermal gradients are involved in the laser cladding process, the various cladding strategies can lead to different heat cycles and different mechanical properties (Tabernero et al., 2011). Preheating of the substrate material is known to residual thermal stresses, distortion and delamination (Nickel et al., 2001).

The process of redistributing the irradiance and phase of a laser beam is called beam shaping (Fred M. Dickey, 2000). Diffractive, refractive and reflective laser beam shaping optics, masks and holographic filters among others can be used to achieve the beam shape necessary. Gaussian or top-hat beam profiles have been used in LMD, where the powder stream from a coaxial nozzle has a Gaussian distribution (Lin and Hwang, 1999).

It has been seen that powder grains reach the melt pool mostly solid in LMD. Time taken for these powder grains to incorporate into the melt pool depends on the position of initial interaction. For a LMD process with power 1 kW and a Gaussian beam, it was seen that the powder grains that arrive at the centre of the laser spot are incorporated the fastest into the melt pool, and those that arrive further away from the centre of the laser spot float on the surface of the melt pool until they are incorporated. These powder grains also move on the surface on the melt pool, the direction of their movement is dependent on Marangoni flow and the thermal gradients (Siva Prasad et al., 2019).

This paper investigates the general characteristics and differences in the process while using the top-hat and doughnut beam profiles with single direction and meander raster paths for LMD through high-speed imaging.

2. Methodology

Clads were made through LMD using top-hat and doughnut beam profiles. The substrate material was a superstrength alloy steelASTM A579 grade-31 and the powder feedstock was a ferrous carbide system.

For the deposition, a coaxial ring-slit nozzle was used, where the laser beam and shielding gas pass through a central hole and the carrier gas and powder are fed through the slit. Argon was used as both, the shielding and carrier gas.

The focal planes of the laser beam and the powder stream were aligned with the surface of the substrates, which were preheated to 350 ˚C, with laser spot size 9 mm for both beam profiles. A 1070 nm wavelength laser was used, with the powder set to 5 kW and the cladding speed was 0.5 m/min. During cladding, each track overlapped the previous track by 50 % of the width.

For each beam profile considered, top-hat and doughnut, two cladding strategies were used: single direction and meander. In case of the single direction clads, the nozzle returns to its start position after cladding one track, moves by an offset of 50 % of track width and clads in the same direction as the previous track. For the meander clads, the nozzle trajectory is back and forth with a 50 % of track width offset. This can be seen in figure 1.

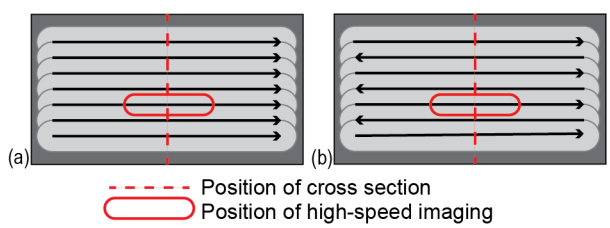

Fig. 1. Illustration of cladding strategies indicating the position of cross sections and high-speed imaging for (a) single direction and (b) meander

The four parameter sets under investigation can be found in Table 1.

Table 1. Experimental parameters

No.	Beam profile	Cladding path	Power (kW)	Cladding speed (m/min)	Deposition rate (g/min)
1	Top-hat	Single direction	5	5	30
2	Top-hat	Meander	5	5	30
3	Doughnut	Single direction	5	5	30
4	Doughnut	Meander	5	5	30

The processes were filmed using a high-speed imaging camera at a frame-rate of 10,000 frames per second (fps). To provide enough light, pulsed laser illumination with wavelength 808 nm and peak power 500 W was used. A narrow bandwidth filter matching the wavelength of the illumination laser blocked out the wavelength of the process light. The camera was inclined at 30˚ to capture the process. The set-up can be found in figure 2.

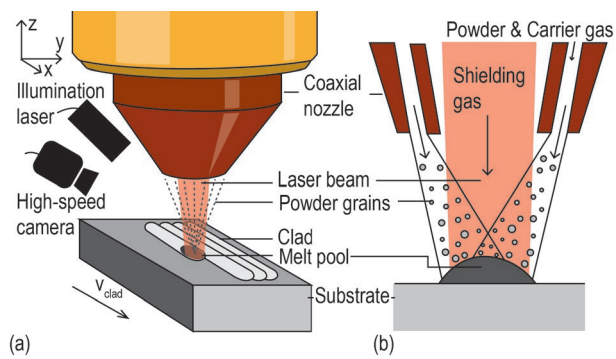

Fig. 2. Schematic illustration of (a) experimental setup and (b) the cross section of the process

The high-speed videos were played back at lower frame rates to observe the details of the process. Observations about the melt pool behaviour, powder flow and catchment were made through these videos. Cross sections of the specimen were made from the centre of the 10 cm long specimen and macrographs were taken to study the variation of dilution. Positions of the cross sections and the high-speed videos made are described in figure 1.

3. Results and Discussion

Successful clads were made using all four experimental parameters listed in table 1. No cracks were formed.

High-speed videos of the studied processes revealed that the general characteristics of the four clads are similar. Figure 3 shows a frame from clad 1 (top-hat, single direction) with a camera angle of 8˚ from the horizontal. It can be seen that the melt pool forms under the laser spot. In the centre of the laser spot, where the powder focus is positioned, an island of unmelted powder grains is formed.

Figure 4 shows a closer view of the melt pool in the top-hat single direction cladding process, with camera

angle 30˚. The island of powder grains, slowly integrates into the melt pool. Some of the powder grains that impact this island ricochet and are not integrated in the clad. It can also be seen that some of the powder grains from this island melt together into a droplet, which either integrates into the melt pool or forms spatter.

This island of powder has not been seen in literature, and previous studies have shown that the powder grains that arrive at the centre of the laser spot are most likely to integrate into the melt pool and integrate faster than those that arrive elsewhere in the melt pool for a Gaussian beam (Siva Prasad et al., 2019). It would be beneficial to use a Gaussian beam to reduce the size or completely eliminate the powder island.

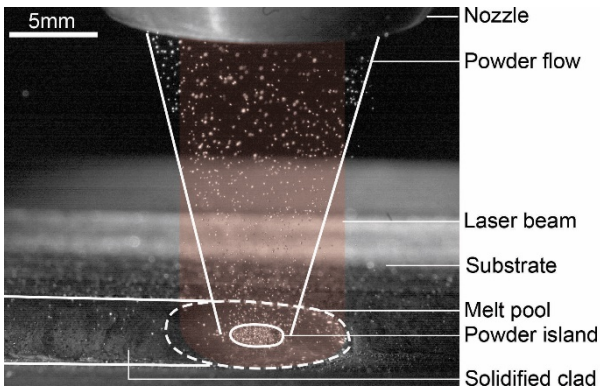

Fig. 3. A frame from high-speed imaging showing an overview of the process

Powder grains that arrive at the melt pool outside of the island, are caught in the melt, may float on the surface of the melt pool until they integrate into the melt. During this period of floating, they move away from the centre of the laser spot towards the edges of the melt pool, before integrating with the melt, as described in figure 4. It can be seen that some powder grains that reach the solidifying edge of the melt pool before fully integrating with the melt, and remain as surface roughness on the clad.

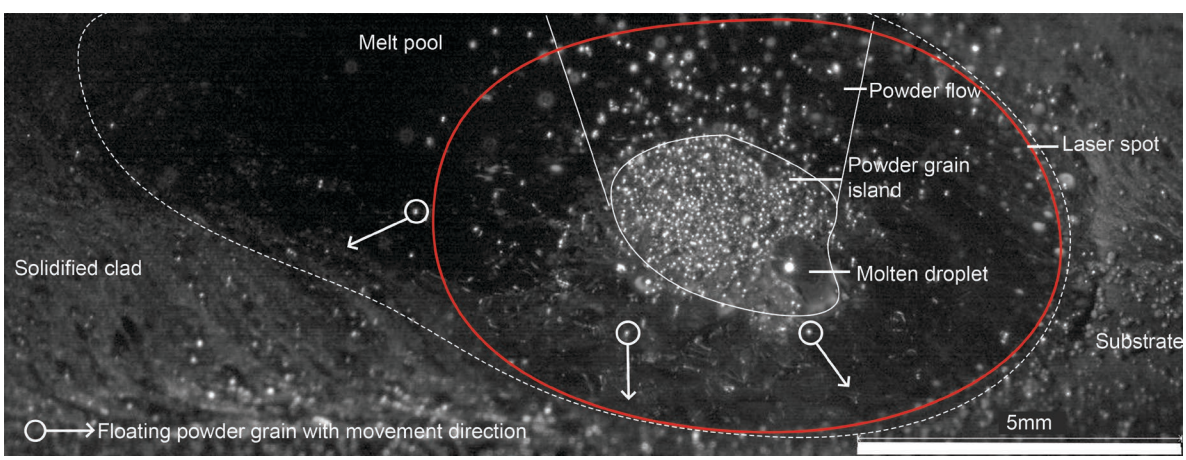

Fig. 4. Frame with a close up image of the melt pool from high-speed imaging

Frames from videos recorded using the four experimental parameters from table 1 can be found in figure 5. Comparison of videos led to the following observations:

The size and behaviour of the melt pool for clads made with meander paths for the top-hat beam was seen to be larger than that of the single direction clads. The size of the powder island remained approximately the same.

For single direction cladding with the doughnut beam, the melt pool was significantly smaller and the powder island larger when compared to the single direction cladding with the top-hat beam.

The size of the melt pool was larger and that of the powder island was smaller when using the meander cladding path with the doughnut beam as compared to single direction cladding. However, the size of the melt pool was still smaller than that formed during cladding with a top-hat beam and meander path.

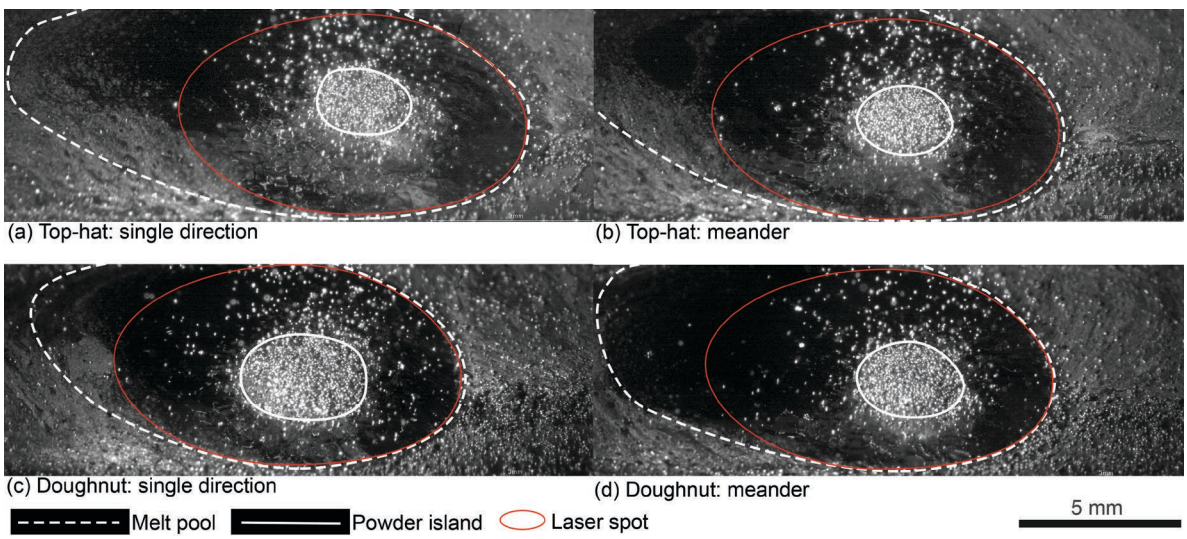

Fig. 5. Frames from high speed imaging videos of the (a) top-hat beam with the single direction path, (b) top-hat beam with the meander path, (c) doughnut beam with the single direction path, and (d) doughnut beam with the meander path laser cladding.

When the meander cladding path is used, cladding is done in a back and forth path. This heat cycle would result in a higher temperature as compared to the single direction cladding path, where the nozzle makes a return movement before cladding any subsequent tracks. The higher temperature of the solidified clads implies a shallower temperature gradient between the melt pool and the surrounding metal, resulting in a larger melt pool.

The doughnut beam has a low intensity at the centre of the laser spot, implying less laser intensity available to melt the powder grains forming the island. On using the meander path, the increased heat available helps in reducing the size of the powder island.

Figure 6 compares the cross section macrographs of the four clads made. The dilution seen in the clads made in the single direction is uneven. The variation is seen to be lower in case of the clads made using the meander path. In both cases, dilution seen in the doughnut beam varies more than that of the top-hat beam.

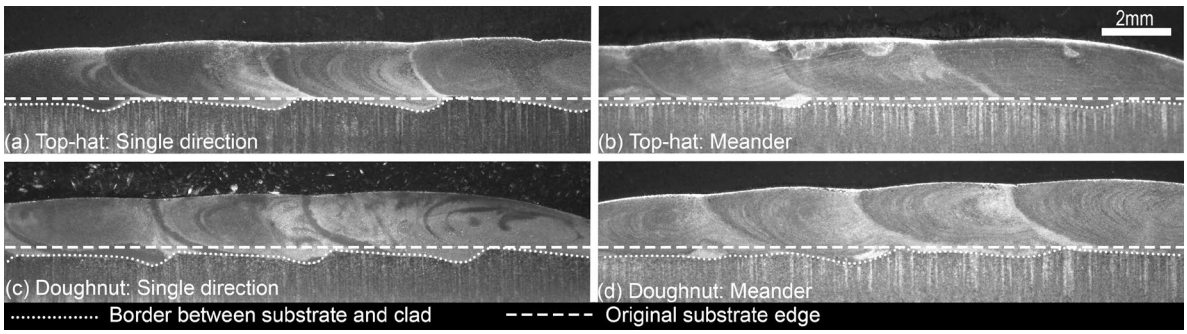

Fig. 6. Optical macrographs of the cross-section of the clads using: (a) top-hat beam with the single direction path, (b) top-hat beam with the meander path, (c) doughnut beam cladded with single direction path, and (d) doughnut beam with the meander path.

4. Conclusions

Characteristics of a high deposition rate Laser Metal Deposition process were studied using the top-hat and doughnut beam profiles with single direction and meander cladding paths by observing the high-speed imaging and cross section macrographs.

An island of unmelted powder can be formed in the centre of the laser spot which slowly incorporates into the melt pool for the top hat and doughnut beam profiles. A Gaussian beam could be more suitable to avoid this island.

The size of the melt pool varies based on the beam profile and cladding paths used. The largest melt pool was seen for the top-hat beam with meander path and the smallest was in the case of the doughnut beam with single direction cladding path.

For lowest and most even dilution, the preferred combination for the chosen parameters is a top-hat beam with a meander cladding path.

Acknowledgements

The work concerning this paper was funded by VINNOVA project ÖVERLAG no. 2017-03240 and EU ERDF, Interreg Nord, project C3TS no. 304-10694-2017.

References

Fred M. Dickey, S.C.H., 2000. Laser Beam Shaping, Optical Science and Engineering. CRC Press. https://doi.org/10.1201/9780824741631

Koshy, P., 1985. Laser Cladding Techniques For Application To Wear And Corrosion Resistant Coatings, in: Jacobs, R.R. (Ed.), Proc. SPIE 0527, Applications of High Power Lasers. p. 80. https://doi.org/10.1117/12.946398

Lin, J., Hwang, B.-C., 1999. Coaxial laser cladding on an inclined substrate. Opt. Laser Technol. 31, 571–578. https://doi.org/10.1016/S0030-3992(99)00116-4

Nickel, A.H.., Barnett, D.M.., Prinz, F.B., 2001. Thermal stresses and deposition patterns in layered manufacturing. Mater. Sci. Eng. A 317, 59–64. https://doi.org/10.1016/S0921-5093(01)01179-0

Siva Prasad, H., Brueckner, F., Kaplan, A.F.H., 2019. Powder catchment in laser metal deposition. J. Laser Appl. 31, 022308. https://doi.org/10.2351/1.5096130

Tabernero, I., Lamikiz, A., Martínez, S., Ukar, E., Figueras, J., 2011. Evaluation of the mechanical properties of Inconel 718 components built by laser cladding. Int. J. Mach. Tools Manuf. 51, 465–470. https://doi.org/10.1016/j.ijmachtools.2011.02.003